

Electronic Supplementary Information

Self-assembled ZnO microspheres coated with carbon dots-doped CoNi LDH wrinkled films as electrochemical sensors for highly sensitive detection of hydrazine

Yu Zhang, Jiaying Wu, Shan Zhao, Xin Tang, Zhiyuan He, Ke Huang, Huimin Yu, Zhirong Zou* Xiaoli Xiong*

College of Chemistry and Materials Science, Sichuan Normal University, Chengdu, Sichuan 610068, China

*Corresponding author: zouzhirong@sicnu.edu.cn; xiongxiaoli2000@163.com

1. Experimental Details

1.1 Materials

Nickel nitrate hexahydrate ($\text{Ni}(\text{NO}_3)_2 \cdot 6\text{H}_2\text{O}$), cobalt nitrate hexahydrate ($\text{Co}(\text{NO}_3)_2 \cdot 6\text{H}_2\text{O}$), zinc acetate, citric acid (CA) and anhydrous ethanol all bought from China Chengdu Kelong Reagent Co. Ltd. Ethylene glycol (EG), ethylenediamine and Hydrazine monohydrate ($\text{N}_2\text{H}_4 \cdot \text{H}_2\text{O}$, 98%) from Sinopharm Chemical. Nickel foam (NF) was purchased from Ce Tech Co., Ltd. Before use, the NF was immersed in a 3M hydrochloric acid solution for 15 min to remove the surface oxide layer. Subsequently, it was washed in an acetone ultrasonic bath for 15 min to remove the oily foam. Finally, it was rinsed three times with ethanol and deionized water, respectively. All chemical reagents used in the experiments were of analytical grade and ready for use without

further purification. Milli-Q ultrapure water (18.25 M Ω) was used for all experiments.

1.2 Preparation of NCDs

NCDs was synthesized from the previous report¹. Typically, citric acid (10.50 g) and ethylenediamine (3.35 mL) were dissolved in deionized water (100 mL). The solution was then transferred to a tetrafluoroethylene autoclave (Teflon-lined, stainless-steel autoclave) and heated at 200 °C for 5 hours. After the reaction was finished, it was cooled naturally to room temperature. The resulting solution was purified and dried to obtain a solid.

1.3 Preparation of ZnO

ZnO microspheres were synthesized on NF by a simple one-step hydrothermal method.² Dissolve 0.80 g of zinc acetate into 30 mL of ethylene glycol. After sufficient dissolution, the pretreated NF and the mixed solution were transferred to a tetrafluoroethylene autoclave and kept at 170 °C for 16 h. Then, it was washed several times with ethanol and water and dried at 60 °C for 3 h.

1.4 Preparation of ZnO@CoNi LDH-NCDs

CoNi LDH-NCDs thin films were prepared by electrodeposition at room temperature. Briefly, Ni(NO₃)₂·6H₂O, Co(NO₃)₂·6H₂O and NCDs powder (5, 20, 40, 60, 80, and 100 mg) were dissolved in ultrapure water to form a mixed solution. The electrodeposition was carried out at a constant potential of -1.0 V, where ZnO was used as the working electrode, and Hg/HgO and platinum wire were used as the reference and counter electrode, respectively. ZnO@CoNi LDH-NCDs samples were obtained. To explore the effect of electrodeposition time on catalyst performance the

electrodeposition time was set to 20 s, 50 s, 100 s, 150 s, 200 s, and 300 s, respectively. For comparison, ZnO@CoNi LDH-NCDs were prepared without the addition of NCDs powder.

1.5 Determination of hydrazine in leachate and water samples

Hydrazine was measured in three different water samples: tap water, lake water and leachate. The leachate samples used in this study were collected from a membrane bioreactor (MBR) at a large anaerobic landfill in southwest China and treated by UV/Fe⁰/H₂O₂ process for 60 min. For the quantification of hydrazine, a standard addition method was used, adding an appropriate amount of hydrazine to the sample. Before detection, we first filter the water samples (tap water, lake water) with a 0.22 μm filter to remove some suspended solids. Store water samples in the refrigerator immediately after collection.

1.6 Characterizations

XRD data were acquired from a D/MAX-RB X-ray diffractometer with Cu Kα radiation (40 kV, 30 mA) of wavelength 0.154 nm (Rigaku, Japan). scanning electron microscope (SEM) measurements were performed on a MERLIN Compact scanning electron microscope (Carl Zeiss AG, Germany). High resolution transmission electron microscopy (HRTEM) images were collected by FEITecnai G2 F30 TEM at 300 kV. X-ray photoelectron spectroscopy (XPS) measurement of the total spectrum and spectrum of each element was tested by ESCALABMK II X-ray photoelectron spectrometer using Mg as the excitation source. Infrared (IR) spectroscopy was performed on a VERTEX 70 FT-IR spectrometer. Photoluminescence (PL) emission,

and PL excitation spectra were acquired on an F-4600 instrument. Ultraviolet and visible spectrophotometry (UV-Vis) was acquired on a UV2310II.

1.7 Electrocatalytic measurements

The electrochemical measurement tests were conducted on an electrochemical work station (CHI660E, Shanghai Chenhua, China) in a conventional three-electrode cell. The system uses NF(1×1cm²), Hg/HgO electrode and Pt as working electrode, counter electrode and reference electrode, respectively. The effective area of the working electrode is 0.04cm² (0.2×0.2cm). The measured overpotential was converted to the potential with the reversible hydrogen electrode (RHE) according to $E_{vs\ RHE} = E_{vs\ SCE} + E_{SCE}^{\theta} + 0.059\ pH$. Electrochemically active surface areas (ECSA) were calculated by dividing the doublelayer capacitance (C_{dl}) with specific capacitance of these samples. The ECSA was calculated using the formula: $ECSAs = C_{dl}/C_s$, where C_s is the specific capacitance of per unit area for sample identical electrolyte Conditions, C_{dl} was determined by cyclic voltammograms (CVs) with multiple scan rates in non-faradaic potential region. For the electrochemical impedance spectroscopy (EIS) measurement, the frequency range was 10⁵ to 0.1 Hz.

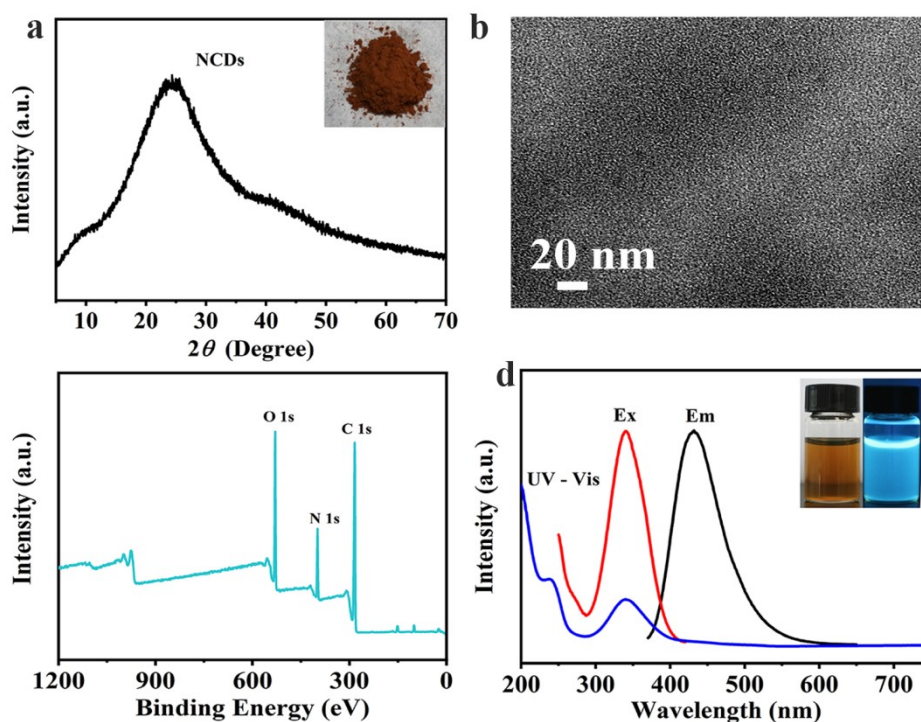


Fig. S1 (a) Experimental XRD patterns for NCDs. (b) The TEM image of NCDs. (c) Survey XPS spectrum of as synthesized NCDs. (d) UV-vis, PL emission, and PL excitation spectra of as synthesized NCDs, Insets show photographs of NCDs in aqueous solution under visible (left) and UV (right) light.

The structure of the NCDs was investigated by X-ray powder diffraction (XRD) (Fig. S1a). The broad diffraction peak around 24.6° corresponds to the (002) diffraction plane of carbon.³ As shown in Fig. S1b, the TEM image shows that NCDs are uniformly distributed with diameters ranging from 4 to 6 nm. X-ray photoelectron spectroscopy (XPS) shows typical peaks for C1s (284.6 eV), N1s (400 eV) and O1s (531 eV) (Fig. S1c). In the UV-vis absorption spectrum (Fig. S1d), the absorption maxima at 238 and 340 nm correspond to the π - π^* and C=O double bonds of the aromatic sp^2 conjugate field, respectively.⁴ Under light excitation at 340 nm, the NCDs exhibit an intense

fluorescent properties at 430 nm, which are the same as the NCDs reported in other literatures.

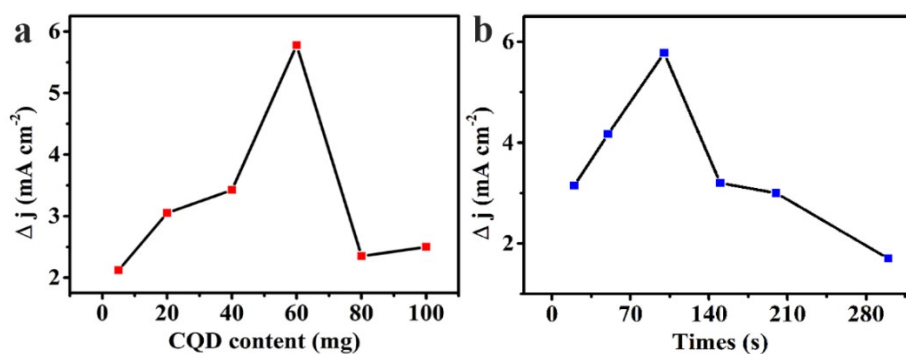


Fig. S2 Optimization of experimental of the ZnO@CoNi LDH-NCDs hydrazine sensor (a) the content of NCDs, (b) the effect of electrodeposition time.

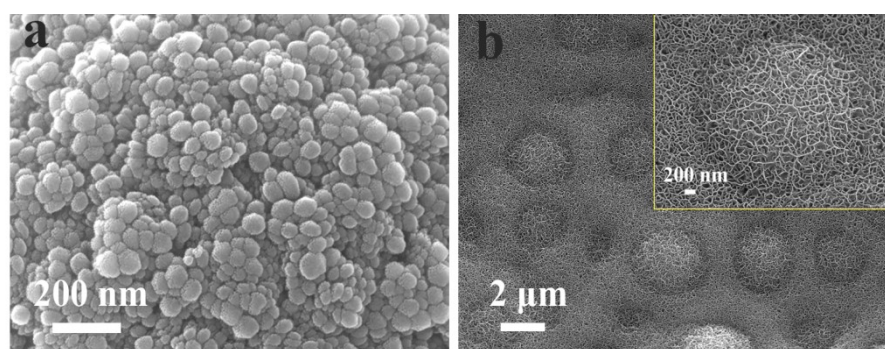


Fig. S3 (a) SEM magnification of ZnO microspheres. (b) SEM images of ZnO@CoNi LDH.

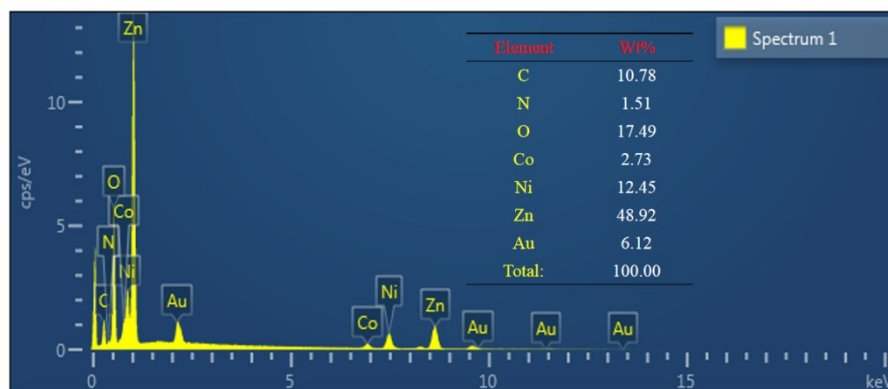


Fig. S4 EDX spectrum of ZnO@CoNi LDH-NCDs.

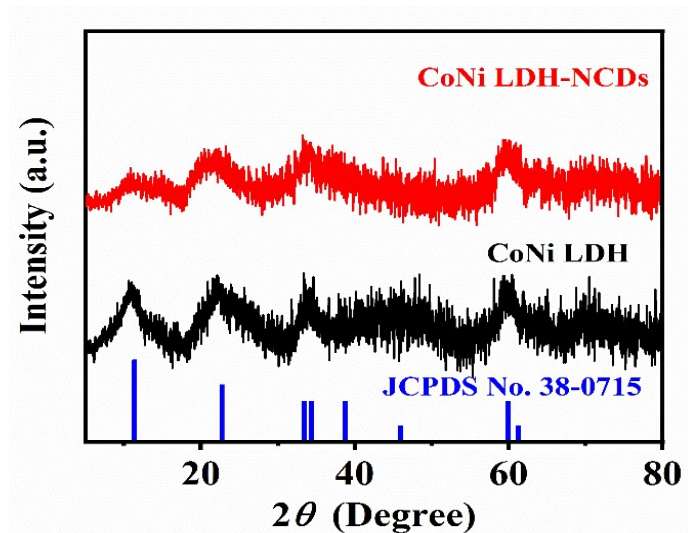


Fig. S5 XRD patterns of CoNi LDH-NCDs and CoNi LDH

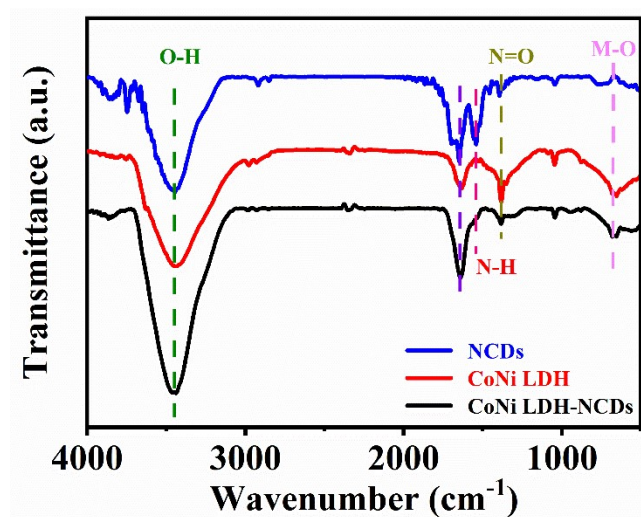


Fig. S6 FTIR spectra of the NCDs, CoNi LDH, and CoNi LDH-NCDs.

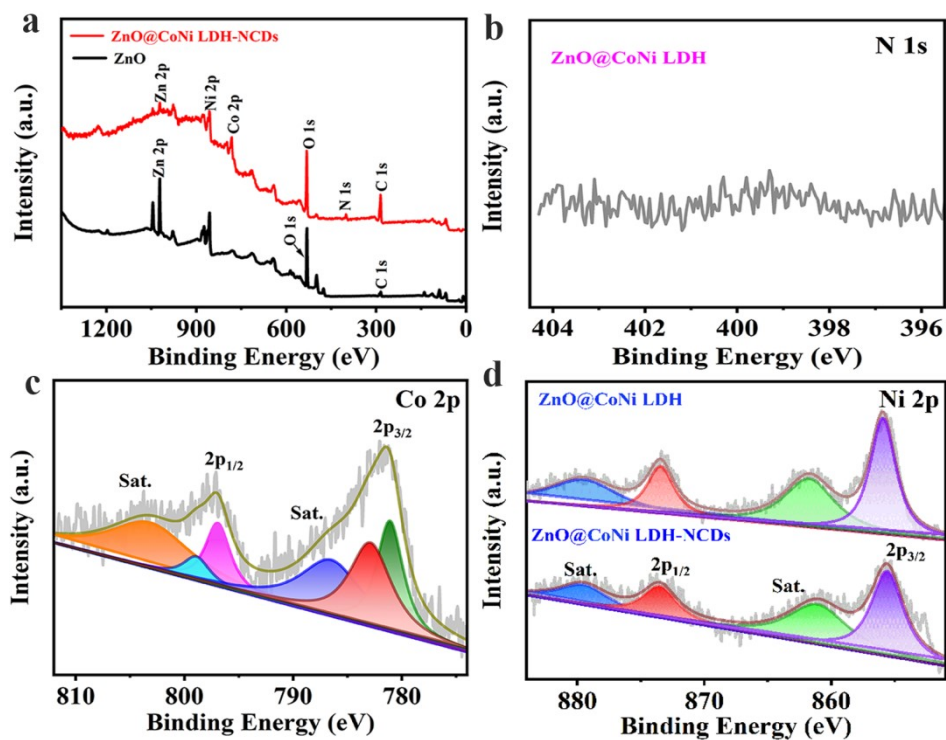


Fig. S7. (a) XPS survey spectrum of the ZnO and ZnO@CoNi LDH-NCDs. (b) N 1s XPS spectrum. (c) Co 2p spectrum and (d) Ni 2p spectrum of ZnO@CoNi LDH-NCDs.

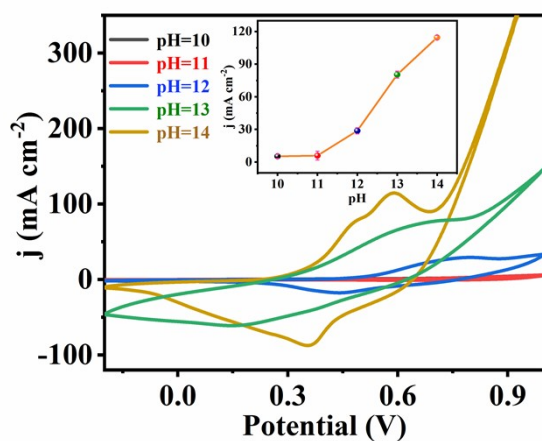


Fig. S8. The CV curves of ZnO@CoNi LDH-NCDs in the presence of 1 mM hydrazine with different pH levels from 10-14 at a scan rate of 50 mV s⁻¹. (Inset: plot of pH vs. anodic peak current.)

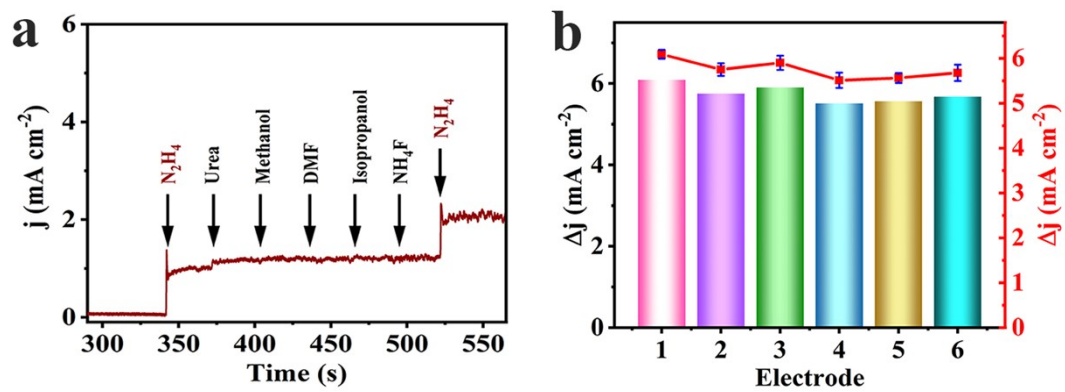


Fig. S9 (a) Amperometric response of 0.6 mM possible interfering substance in the presence of 0.06 mM of hydrazine on ZnO@CoNi LDH-NCDs. (b) The amperometric responses to 1 mM hydrazine at six independently prepared ZnO@CoNi LDH-NCDs.

Table S1. Comparison of performance of different amperometric sensors for determination of hydrazine.

Electrode materials	Sensitivity (μA $\mu\text{M}^{-1} \text{cm}^{-2}$)	Linear range (μM)	LOD (μM)	Refs.
Au/ZnO	0.873	0.2–14.2	0.242	5
PTh/ZnO	1.22	0.5–48	0.207	6
Co ₃ O ₄ /rGO/CC	1.307($\mu\text{A} \mu\text{M}^{-1}$)	5.0–470	0.141	7
chestnut-like NiCo ₂ O ₄	---	1-1096	0.30	8
ZnO nanonail	8.56	0.1–1200	0.2	9
ZnO nanorods-SWCNTs	0.1	0.5-50	0.17	10
Ni(II)/GCE	0.1174	0.5–150	166	11
AuNPs@NiO NSs/NF	17.80	0.2–300	0.04	12
CoOOH	0.101	40-1000	40	13
	0.156	20-1200	20	
NiCo ₂ S ₄ /GCE	0.1791	1.7–7800	0.6	14
NiFe ₂ O ₄ -MWCNTs	100 $\mu\text{A}\mu\text{M}^{-1}$	5-2500	1.5	15
ZnO@CoNi LDH-NCDs	13.04	0.7-4000	0.2	This work

Reference

1. H. Song, M. Wu, Z. Tang, J. S. Tse, B. Yang and S. Lu, *Angew. Chem. Int. Edit.*, 2021, 60, 7234-7244.
2. J. Chao, Y. Chen, S. Xing, D. Zhang and W. Shen, *Sensory Actuat B-Chem.*, 2019, 298, 126927.
3. W. Li, Y. Liu, M. Wu, X. Feng, S. A. T. Redfern, Y. Shang, X. Yong, T. Feng, K. Wu, Z. Liu, B. Li, Z. Chen, J. S. Tse, S. Lu and B. Yang, *Adv. Mater.*, 2018, 30, 1800676.
4. G. Wei, X. Zhao, K. Du, Y. Huang, C. An, S. Qiu, M. Liu, S. Yao and Y. Wu, *Electrochim. acta.*, 2018, 283, 248-259.
5. A. A. Ismail, F. A. Harraz, M. Faisal, A. M. El-Toni, A. Al-Hajry and M. S. Al-Assiri, *Mater. Design*, 2016, 109, 530-538.
6. M. Faisal, F. A. Harraz, A. E. Al-Salami, S. A. Al-Sayari, A. Al-Hajry and M. S. Al-Assiri, *Mater. Chem. Phys.*, 2018, 214, 126-134.
7. Q. Wang, M. Wu, S. Meng, X. Zang, Z. Dai, W. Si, W. Huang and X. Dong, *Adv. Mater. Interfaces*, 2016, 3, 1500691.
8. X. Zhang, Y. Wang, X. Ning, I. Li, J. Chen, D. Shan, R. Gao and X. Lu, *Anal. Chim. Acta*, 2018, 1022, 28-36.
9. A. Umar, M. M. Rahman, S. H. Kim and Y.-B. Hahn, *Chem. Commun.*, 2008, DOI: 10.1039/B711215G, 166-168.
10. K. N. Han, C. A. Li, M.-P. N. Bui, X.-H. Pham and G. H. Seong, *Chem. Commun.*, 2011, 47, 938-940.
11. T. Hosseinzadeh Sanatkar, A. Khorshidi, E. Sohoulfi and J. Janczak, *Inorg. Chim. Acta*, 2020,

506, 119537.

12. W. Wang, Z. Zhao, Q. Lei, W. Zhang, P. Li, W. Zhang, S. Zhuiykov and J. Hu, *Appl. Surf. Sci.*, 2021, 542, 148539.
13. K. K. Lee, P. Y. Loh, C. H. Sow and W. S. Chin, *Biosens. Bioelectron.*, 2013, 39, 255-260.
14. C. Duan, Y. Dong, Q. Sheng and J. Zheng, *Talanta*, 2019, 198, 23-29.
15. B. Fang, Y. Feng, M. Liu, G. Wang, X. Zhang and M. Wang, *Microchim. Acta*, 2011, 175, 145.